A steroid receptor coactivator stimulator (MCB-613) attenuates adverse remodeling after myocardial infarction

Lisa K. Mullany[a,1], Aarti D. Rohira[a,1], John P. Leach[b,2], Jong H. Kim[c,d,2], Tanner O. Monroe[c], Andrea R. Ortiz[a], Brittany Stork[a], M. Waleed Gaber[e], Poonam Sarkar[e], Andrew G. Sikora[f], Todd K. Rosengart[g], Brian York[a], Yongcheng Song[h], Clifford C. Dacso[a], David M. Lonard[a], James F. Martin[c,d,3], and Bert W. O'Malley[a,3]

[a]Department of Molecular and Cellular Biology, Baylor College of Medicine, Houston, TX 77030; [b]Penn Cardiovascular Institute, Perelman School of Medicine, University of Pennsylvania, Philadelphia, PA 19104; [c]Department of Molecular Physiology and Biophysics, Baylor College of Medicine, TX 77030; [d]Cardiomyocyte Renewal Lab, Texas Heart Institute, Houston, TX 77030; [e]Department of Pediatrics, Baylor College of Medicine, Houston, TX 77030; [f]Department of Otolaryngology-Head & Neck Surgery, Baylor College of Medicine, Houston, TX 77030; [g]Department of Surgery, Baylor College of Medicine, Houston, TX 77030; and [h]Department of Pharmacology and Chemical Biology, Baylor College of Medicine, Houston, TX 77030

Contributed by Bert W. O'Malley, September 16, 2020 (sent for review June 23, 2020; reviewed by Chris Glass and Philip W. Shaul)

Progressive remodeling of the heart, resulting in cardiomyocyte (CM) loss and increased inflammation, fibrosis, and a progressive decrease in cardiac function, are hallmarks of myocardial infarction (MI)-induced heart failure. We show that MCB-613, a potent small molecule stimulator of steroid receptor coactivators (SRCs) attenuates pathological remodeling post-MI. MCB-613 decreases infarct size, apoptosis, hypertrophy, and fibrosis while maintaining significant cardiac function. MCB-613, when given within hours post MI, induces lasting protection from adverse remodeling concomitant with: 1) inhibition of macrophage inflammatory signaling and interleukin 1 (IL-1) signaling, which attenuates the acute inflammatory response, 2) attenuation of fibroblast differentiation, and 3) promotion of Tsc22d3-expressing macrophages—all of which may limit inflammatory damage. SRC stimulation with MCB-613 (and derivatives) is a potential therapeutic approach for inhibiting cardiac dysfunction after MI.

myocardial infarction | MCB-613 | fibrosis

Mitigating the pathophysiological impact to cardiac function following myocardial infarction (MI) by preserving functional myocardium and attenuating detrimental remodeling of cardiac tissue subsequent to an acute heart attack is an unmet therapeutic need. Previous work from ours and other laboratories have shown that steroid receptor coactivators (SRCs) are involved in heart development and in mitigating cardiac dysfunction in cardiac injury models (1, 2). We have identified a small molecule activator of SRCs (MCB-613) that selectively and reversibly binds to SRCs as shown by surface plasmon resonance and is a potent SRC stimulator that acts to greatly enhance SRC transcriptional activity with no apparent toxicity in mice (3). Members of the p160 SRC family, SRC-1 (NCOA1), SRC-2 (NCOA2/TIF2/GRIP1), and SRC-3 (NCOA3/AIB1/ACTR/pCIP), interact with nuclear receptors and other transcription factors to drive target gene expression (4) by assembling transcriptional coactivator complexes to increase transcription. SRCs act as primary transcriptional regulators of transcription factor activity necessary for cell proliferation, survival, cell motility, invasion and metastasis, and cell metabolism. SRC-coactivators are widely expressed and function as master regulators of cellular plasticity and cell proliferation both during normal and abnormal growth and during development (5–9). SRCs function as coactivators for the transcription factors for cell signaling and molecular pathways critical for wound healing including, nuclear factor kappa B (NF-κB) (NFKB1) (10), SREBP1 (11), and AP-1 (JUN) (12, 13); this indicates a potential for SRC-targeting drugs pertinent to cell migration, proliferation, and survival-promoting paracrine interactions in tissue injury responses. Pleotropic actions of SRCs range from immune regulation (14) and angiogenesis (15) to maintenance of metabolic regulation in diverse organ systems including the heart (16). Specifically in the heart, recent findings indicate that SRC family members regulate cardiomyocyte function during early cardiac development (17) and in response to cardiac metabolic stress (18).

Cellular plasticity and growth in response to patterning signals associated with organogenesis often are reactivated during tumor progression, tissue regeneration, and wound healing. Specifically in the heart, cardiac fibroblasts undergo phenotypic conversion in response to cardiac injury (19) but respond in ways that are detrimental to cardiac function post-MI (20). Thus, targeting of specific repair events or recapitulation of the embryonic role of SRCs after disease-related tissue damage in the adult heart might be expected to provide therapeutic opportunities for promoting optimal tissue reprogramming and repair. Based on known functions of SRCs in maintenance of cellular pluripotency and promoting plasticity during early heart development, we postulated that MCB-613 could enable wound repair and preservation of cardiac function after an acute MI by reducing the extent of injury-related fibrosis and the subsequent chronic loss of cardiac function associated with noncontracting scar tissue. We thus tested the effect of MCB-613 on the cardiac injury response by administering MCB-613 2 h after ischemic

Significance

We are at an exciting era of identification of the cell and molecular processes necessary for tissue remodeling and repair. Unlike current systemic therapeutics, our studies reveal pharmacologic stimulation of SRCs modulates macrophage and fibrotic reparative cell responses to promote more effective repair and lasting beneficial remodeling after myocardial infarction.

Author contributions: L.K.M., A.D.R., J.P.L., A.G.S., T.K.R., C.C.D., D.M.L., and B.W.O. designed research; L.K.M., A.D.R., J.P.L., J.H.K., T.O.M., A.R.O., B.S., M.W.G., P.S., B.Y., and J.F.M. performed research; Y.S. contributed new reagents/analytic tools; L.K.M., A.D.R., J.P.L., J.H.K., T.O.M., A.R.O., B.S., M.W.G., P.S., J.F.M., and B.W.O. analyzed data; and L.K.M., J.F.M. and B.W.O. wrote the paper.

Reviewers: C.G., University of California, San Diego; and P.W.S., University of Texas Southwestern Medical Center.

The authors declare no competing interest.

[1]L.K.M. and A.D.R. contributed equally to this work.

[2]J.P.L. and J.H.K. contributed equally to this work.

[3]To whom correspondence may be addressed. Email: jfmartin@bcm.edu or berto@bcm.edu.

This article contains supporting information online at https://www.pnas.org/lookup/suppl/doi:10.1073/pnas.2011614117/-/DCSupplemental.

First published November 23, 2020.

injury in a mouse model of MI. Along with measurements of functional cardiac output and damage, we sought to identify the cell-type specific responses responsible for MCB-613's cardioprotective effects by utilizing single cell transcriptomics of cardiac interstitial cells to characterize the effects of SRC stimulation on cardiac function post-MI.

Results

MCB-613 Inhibits Loss of Cardiac Function Post-MI. We reasoned that MCB-613 could ameliorate recovery after ischemia-induced MI. To test this, MCB-613 or vehicle control was administered to mice following myocardial injury induced by a highly experienced surgeon who permanently ligated the left anterior descending (LAD) coronary artery (*SI Appendix*, Fig. S1*A*), a commonly used preclinical MI model for testing cardiovascular therapeutic interventions (21). Two hours post-MI, mice were randomized into two groups that received 20 mg/kg MCB-613 or vehicle control by intraperitoneal injection. Repeat injections were administered every 24 h for six additional days in the immediate post-MI period. Three additional doses were administered at D55-57 post-MI to determine if MCB-613 could further improve cardiac function in the postinjury maintenance phase. Individual mice were followed longitudinally by echocardiography prior to surgery, at 24 h and at 14, 56, and 80 d post-MI. All echocardiography measurements were performed in a blinded fashion. Mice in both treatment groups had an immediate drop in ejection fraction (EF) post-MI (Fig. 1*A*, 24 h post-MI % ejection fraction) and visual evidence of an intact ligation thread and local cardiac tissue blanching at the time of harvest, indicating successful coronary artery ligation. EF decreased to an average of 35% in control ($n = 10$) and 42% in MCB-613-treated ($n = 11$) mice 24 h post-MI ($P = 0.9$ not significant). In control mice, EF continued to decline and was at its lowest point at 80 d post-MI, indicating progressive loss of cardiac function over time, as is expected after an MI. In contrast, MCB-613-treated mice had an average EF of 50% at 14 d post-MI that was maintained above an EF of 43% until the final measurement at 80 d post-MI (Fig. 1*A*). These data indicate that after the initial ischemic insult, MCB-613 inhibited a further decline in cardiac function and provided protection from ischemic injury (Fig. 1*A*). In addition, our data indicate that the early myocardial protective effects of MCB-613 were long-lived and progressive loss of cardiac function was diminished. Repeat injections given for 3 d in week 8 (D55-57) did not further improve EF, suggesting that the beneficial effect of MCB-613 occurred earlier in the post-MI period. An early dosing strategy was tested to determine if immediate and sustained improvement starting 24 h post-MI could be achieved with three injections administered every other day (*SI Appendix*, Fig. S1*B*). Three doses given 2 h, 2 d and 4 d post-MI significantly improved cardiac function 24 h and 2 wk post-MI, indicating daily MCB-613 is not required for improved cardiac function.

MCB-613 Inhibits Fibrosis and Reduces Infarct Size. Serial sections from apex to the ligation were stained with picrosirius red to evaluate the degree of fibrosis 6 wk post-MI (*SI Appendix*, Fig. S1*C*). All

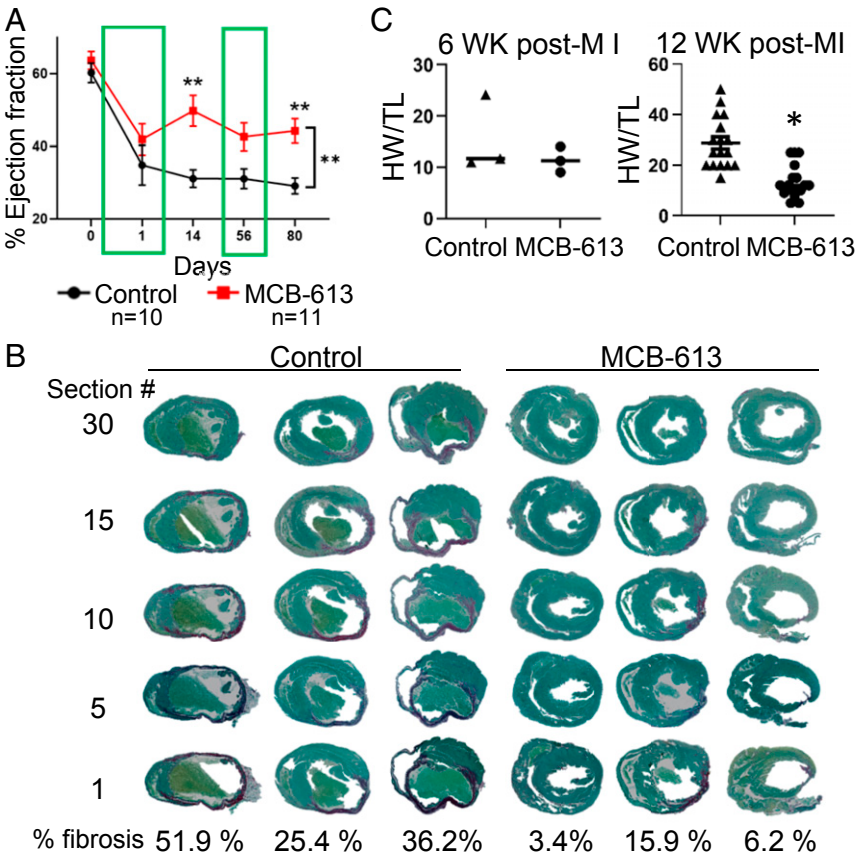

Fig. 1. The SRC-3 activator MCB-613 attenuates loss of cardiac function post-MI. (*A*) Ejection fraction was measured by echocardiography at the indicated times. Values shown are mean ± SEM; two-way ANOVA with repeated measures. $n = 10$ control and $n = 11$ MCB-613. Day 14 $^{**}P$ 0.0078. Day 80 $^{**}P = 0.008$. (*B*) Control-treated hearts ($n = 3$) and MCB-613-treated hearts ($n = 3$) stained with picrosirius red. Quantification of percent fibrosis. Student's *t* test for fibrosis ($^{*}P = 0.03$). (*C*) Values shown are mean ± SEM; Student's *t* test for HW/TL ($n = 6$); ($^{*}P = 0.03$).

sections (sections 1, 5, 10, 15, and 30) in control hearts ($n = 3$) 6 wk post-MI had remodeled scars and fibrosis (36%, 51%, and 26%) (Fig. 1*B*). Considerably less fibrosis was observed in hearts from MCB-613-treated animals ($n = 3$) (16%, 3%, and 6%), indicating MCB-613 attenuates the extent of post-MI remodeling. Similar to 6 wk post-MI, hearts from MCB-613-treated mice 12 wk post-MI showed less fibrosis in the apex region (*SI Appendix*, Fig. S1*D*). Heart weights and tibia lengths were measured in mice harvested at 6 and 12 wk post-MI ($n = 6$) (Fig. 1*C*). A decrease in heart weight/tibia length (HW/TL) indicates MCB-613 attenuated the MI-induced hypertrophic compensatory response at 12 wk post-MI. Taken together, these results demonstrate that MCB-613 inhibits key molecular and cellular features of progressive loss of cardiac function.

In support of early myocardial protection, apoptotic cleaved caspase-3 stain (*SI Appendix*, Fig. S2*A*) is reduced 1 and 3 d post-MI with MCB-613 treatment, indicating MCB-613 diminished the early apoptotic response. Consistent with reduced apoptosis 3 d post-MI, electron micrographs of MCB-613-treated hearts exhibited less disorganization of myofibrillar structure with abnormal mitochondrial cristae (*SI Appendix*, Fig. S2*B*). Using smooth muscle actin (SMA) immunostaining, we assessed myofibroblast differentiation in tissues sections from hearts 3 d post-MI (*SI Appendix*, Fig. S2*C*). Three days post-MI, SMA was decreased in the border zones in hearts from MCB-613-treated mice compared to controls, suggesting MCB-613 attenuates myofibroblast differentiation. Cardiac positron emission tomography (PET) imaging provided a qualitative assessment of myocardial viability in live mice. Improved 18F-fluorodeoxyglucose (18F-FDG) uptake in the infarct zone indicates that MCB-613 preserves healthy myocardium 2 wk post-MI (*SI Appendix*, Fig. S2*D*). Taken together, these

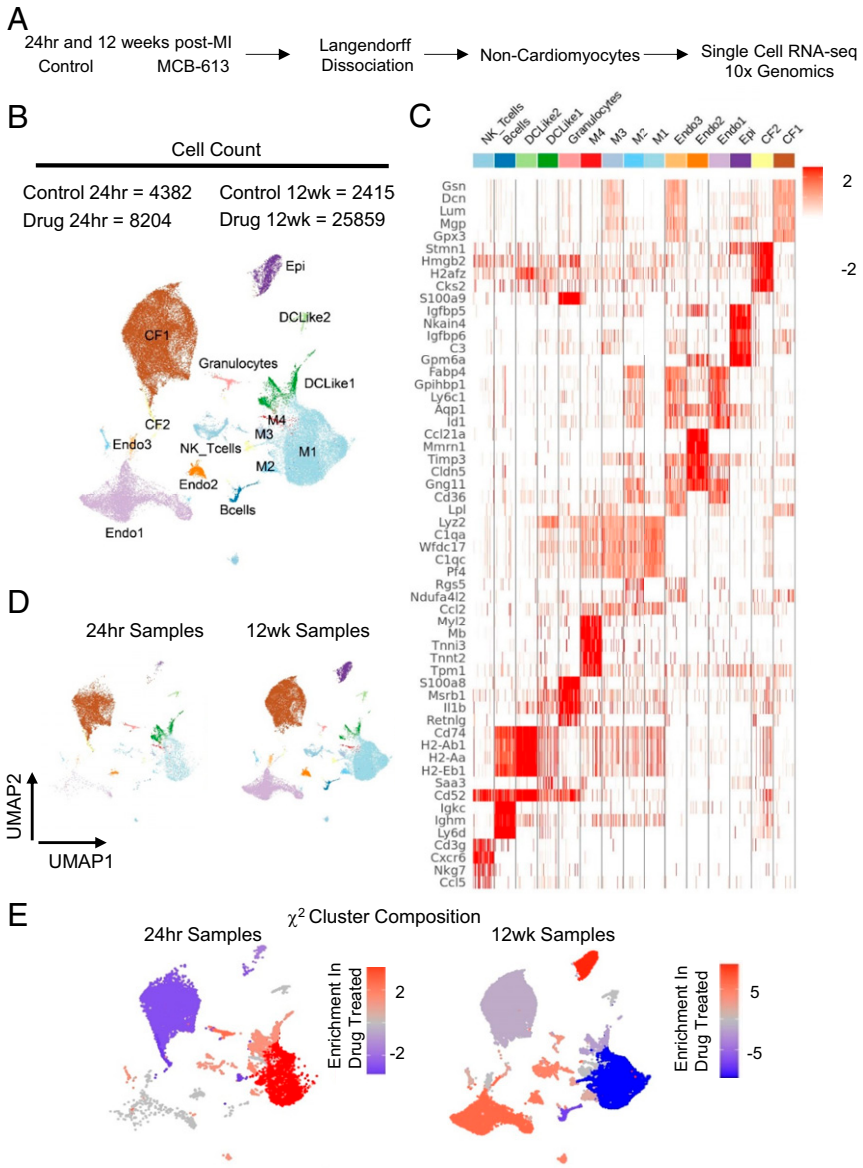

Fig. 2. RNA transcriptional profiling of cardiac cells 24 h and 12 wk post-MI. (*A*) Schematic representation of isolation procedures to obtain non-cardiomyocytes for single cell RNA-seq analysis from control-treated and MCB-613-treated mice 24 h and 12 wk post-MI. $n = 2$ hearts/group. (*B*) UMAP plot of all cell populations identified by unsupervised clustering of single cell transcriptional data. Each dot indicates a single cell. Nonmacrophage immune cells (DC-like 1to 3), B cells, T cells, NK cells, granulocytes, macrophages (M1 to 4), endothelial cells (Endo1 to 3), cardiac fibroblasts (CF1 to 2), and epicardial cells. (*C*) Heat map of top differentially expressed genes in each cell cluster. (*D*) UMAP plot of subclustered cells at 24 h and 12 h. (*E*) The χ^2 cluster composition analysis of cells from MCB-613 compared to control at 24 h and 12 wk post-MI.

findings indicate transient treatment with MCB-613 results in improved heart function with less pathologic remodeling post-MI.

MCB-613 Promotes Beneficial Cardiac Interstitial Remodeling Post-MI. In the heart, interstitial cells such as fibroblasts, immune cells, and endothelial cells play an important role in the injury response. We used single cell transcriptomic profiling (sc-RNA-seq) to investigate interstitial cellular responses in MCB-613-treated mice 24 h and 12 wk post-MI.

For the 24 h collection point, mice were injected 2 h post-MI and hearts were harvested 24 h post-MI for single cell isolation. For the 12 wk collection point, we used the same injection protocol as the echo study with a later collection point. Mice were injected 2 h post-MI and for 6 consecutive days and again at days D55-57 post-MI. Metabolically active, viable, single cell suspensions of noncardiomyocytes were prepared from whole hearts following Langendorff perfusion (Fig. 2*A*). We captured 50,013 cells that were plotted using graph-based clustering, followed by dimensionality reduction using Uniform Manifold Approximation and Projection (UMAP) (22), and revealed distinct cell clusters based on their top differentially expressed genes (Fig. 2 *B* and *C*).

Individual cell clusters ranged from 328 to 24,004 cells. Major cell types consisted of macrophages, dendritic cells (DC)-like cells, B cells, T cells, natural killer (NK) cells, fibroblasts, endothelial cells and epicardial cells. Clusters were grouped and quantified at each time point to discern cell type differences in hearts from MCB-613-treated mice compared to controls at 24 h and 12 wk post-MI (Fig. 2*D* and figure *SI Appendix*, Fig. S3*A*). Cardiac fibroblasts (65%) were the most prevalent cell type 24 h post-MI followed by nonmacrophage immune cells (DC-like1-3, B cells, T cells, NK cells, and granulocytes) (16%), macrophages (M1-4) (15%), and endothelial cells (3%). At 12 wk post-MI, hearts consist of similar proportions of fibroblasts (37%) and macrophages (M1-4) (32%) followed by endothelial cells (23%) along with a smaller representation of nonmacrophage immune cells (DC-Like1-3, B cells, T cells, NK cells, and granulocytes) and epicardial cells (3%) (*SI Appendix*, Fig. S3*A*).

To determine if MCB-613 changes the abundance of different cardiac cell types, we performed a χ^2 analysis on normalized cell counts (Fig. 2*E*). At 24 h post-MI, MCB-613-treated hearts had an increased representation of all macrophage subtypes (M1-4), followed by DC-Like1, granulocytes, and NK-T cells, and a decreased representation of fibroblasts and endothelial cells, suggesting that drug treatment promotes the enrichment of myeloid-derived monocytes either through recruitment or proliferation along with decreased fibroblast cell counts. At 12 wk post-MI, we observed an increase in endothelial cells and a decrease in macrophage cell populations while maintaining improved cardiac function post-MI, indicating reduced inflammation at 12 wk. Cell population shifts in cardiac fibroblasts and macrophages 24 h post-MI are consistent with a decrease in the myofibroblast marker SMA staining at 3 d (See *SI Appendix*, Fig. S2*C*) and fibrosis 6 wk post-MI (Fig. 1*D*). Overall, these data indicate MCB-613 effects on fibroblast and macrophage functions contribute to improved post-MI injury response. Together, these data suggest that improved cardiac function following administration of MCB-613 after ischemic injury is associated with decreased fibroblast populations and increasing macrophage, granulocyte, and NK-T cell numbers.

MCB-613 Attenuates Fibroblast Differentiation 24 h Post-MI. Heterogeneous populations of fibroblasts in the infarct zone arise through a combination of migration, proliferation of existing fibroblasts, or differentiation of cells into activated fibroblasts and myofibroblasts (23, 24). We next explored the fibroblast population for transcriptional differences induced by MCB-613 at 24 h post-MI. The 24-h fibroblast population from Fig. 2 was separated, reclustered, and plotted using UMAP. Two-color UMAP of fibroblasts comparing drug and control-treated hearts show differences in cell composition indicating MCB-613 affects the fibroblast injury response after treatment (Fig. 3*A*). To measure changes in cell number, we performed χ^2 statistical analysis of the cardiac fibroblast clusters and found that three fibroblast clusters are enriched while the five remaining clusters are diminished in MCB-613-treated hearts compared with controls (Fig. 3*B*). Fibroblast clusters, defined by their top differentially expressed marker genes, are classified into eight major groups (Fig. 3 *B* and *C*). Cardiac fibroblasts in cluster 1 (CF1) are marked by expression of peptidase inhibitor 16 (*Pi16*), CF2 fibroblasts express *Apoe*, CF3 fibroblasts selectively express matrix metalloprotease 3 (*Mmp3*), CF4 fibroblasts express the fibrogenic connective tissue growth factor (*Ctgf*), and CF5 fibroblasts express the high mobility group protein 2 (*Hmgb2*) transcription factor.

To determine if changes in cell composition are indicative of changes in cell differentiation, we plotted all fibroblasts along a cellular trajectory through pseudotime using monocle (2.0) by inputting the differentially expressed genes between MCB-613-treated fibroblasts and control (Fig. 3*D*). In the 24 h post-MI hearts, we found fibroblast subclusters CF2, CF3, and CF7, on the left position of the trajectory with a high expression of *Saa3*, while the transitioning clusters CF1, CF6, and CF8, expressing *Ei4a1, Hspa8, Cy61, Uap1, Hspa5, Ugdh,* and *Tnfaip6*, positioned in the middle, followed by clusters CF4 and CF5, differentially expressing *Has1,Ctgf, Serpine1, Ccl4, Angptl4, Ccl2, Inhba, and Timp1,* characterize fibroblasts toward the right of trajectory (differentiated) state (Fig. 3*D*). *Lpl* cells at early pseudotime likely represent a recently reported lipoprotein lipase (LPL)-expressing resident cardiac fibroblast population vulnerable to depletion in mouse hearts 3 d post-MI (25) while *Ctgf* and *Hmgb1* cells at the right position represent injury-responsive fibroblasts associated with fibrosis.

In conjunction with the UMAP in Fig. 3*A*, we find that MCB-613-treated CFs enrich toward the left, while control CFs are more enriched toward the right (Fig. 3*E*). Proinflammatory genes *Ccl2, Ctgf, Serpine1, and Inhba* are differentially enriched in control fibroblasts (Fig. 3*E*). We examined through Gene Ontology (GO) all differentially expressed genes and found that the GO term: cellular response to interleukin 1 (IL-1) was the most overrepresented category in 24-h post-MI fibroblasts, suggesting early IL-1 signaling controls post-MI fibroblast differentiation (Fig. 3*F*). Additional GO terms related to fibroblast functions included positive regulation of collagen biosynthesis and cellular response to growth factor stimulus. Overall, these results suggest that MCB-613 may act through IL-1 signaling pathways and extracellular matrix-remodeling responses to alter the fibroblast injury response in hearts 24 h post-MI.

MCB-613 Promotes Enrichment of Anti-Inflammatory Macrophages. We explored macrophage changes in MCB-613-treated hearts 24 h post-MI. Clusters M1-4 from Fig. 3 were separated, reclustered, and replotted. Macrophage UMAP labeled by sample origin and χ^2 analysis of macrophage subclusters show differences in cell type composition between cardiac macrophages from control-treated compared to MCB-613-treated mice, indicating MCB-613 changes the macrophage injury response 24 h post-MI (Fig. 4*A*). Macrophage clusters 24 h post-MI are defined by distinct expression of C-C chemokine receptor type 2 (*Ccr2*) and the M2-like macrophage marker *Cbr2* (Fig. 4*B*) χ^2 analysis indicates that the CCR2 negative macrophage cluster is enriched while the CCR2 positive macrophage cluster is suppressed in response to MCB-613 compared to control. It has been reported that CCR2 negative cardiac macrophages inhibit monocyte recruitment and promote healing while CCR2 positive macrophages promote inflammation following MI (26). In addition to CCR2 expression, macrophage clusters were further defined by expression of their top five expressed genes (Fig. 4*B*).

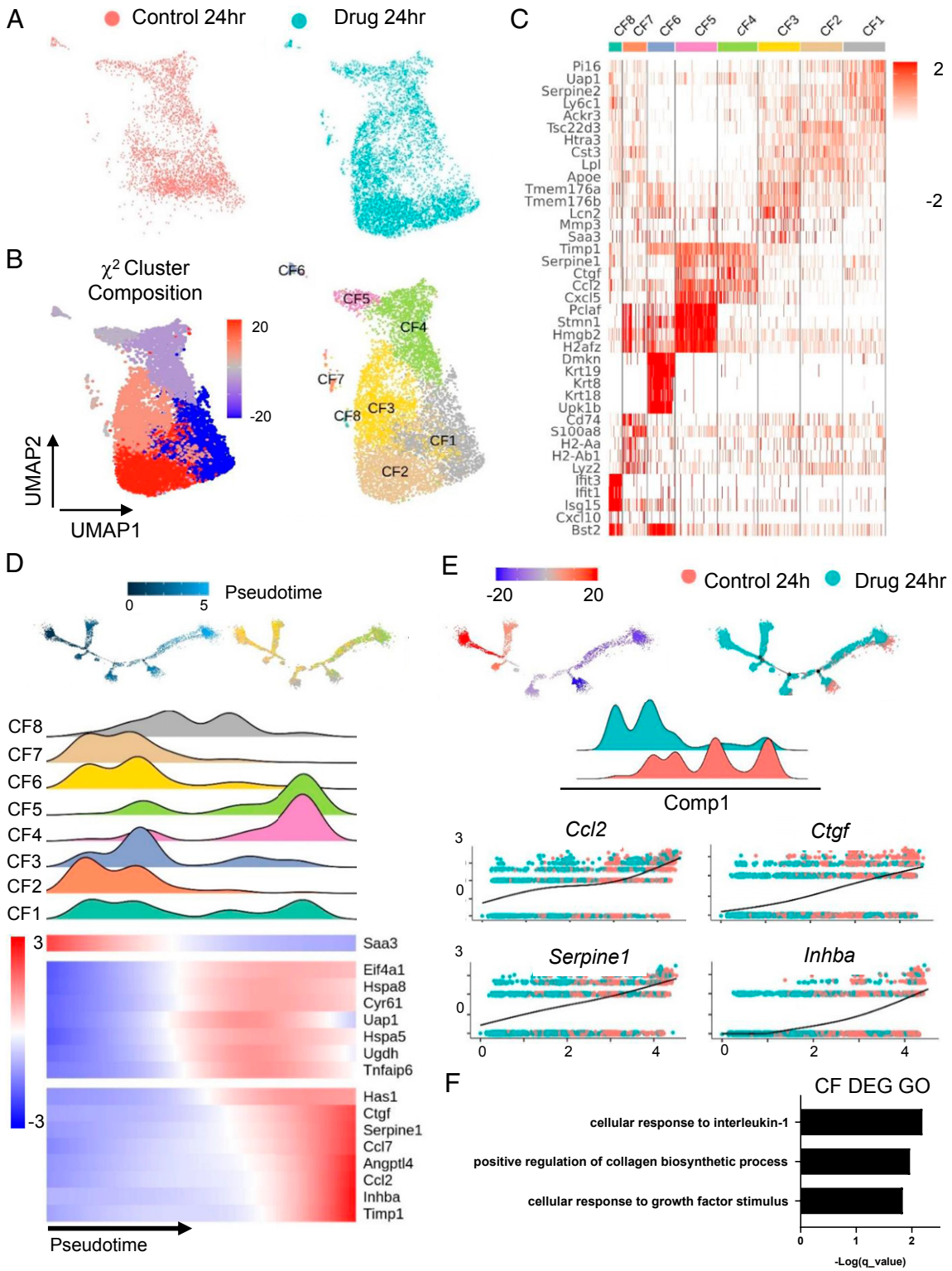

Fig. 3. Single cell analysis of fibroblast cells 24 h post-MI reveals that the MCB-613 protective response is associated with decreased fibroblast differentiation, decreased fibrosis, and Il-1 response. (*A*) UMAP plot of fibroblasts from control (salmon) and MCB-613 (aqua) 24 h post-MI. (*B*) χ^2 cluster composition analysis of subclustered fibroblasts from MCB-613 compared to control at 24 h post-MI (*Left*). UMAP plot of fibroblast subclusters 24 h post-MI (*Right*). (*C*) Heat map showing top five differentially expressed genes. (*D*) Pseudotime trajectory for cardiac fibroblasts 24 h post-MI (*Left*). Pseudotime trajectory colored according to subcluster identity (*Right*). Density plots according to fibroblast subclusters and heatmap showing dynamics of gene expression for subclusters across the trajectory (*Bottom*). (*E*) Pseudotime trajectory colored according to χ^2 cluster composition (*Left*) and treatment condition (*Right*). Density plot according to treatment condition. Gene expression trends for individual genes across the pseudotime trajectory (*Bottom*). (*F*) GO term analysis of differentially expressed genes from fibroblasts in control compared to MCB-613.

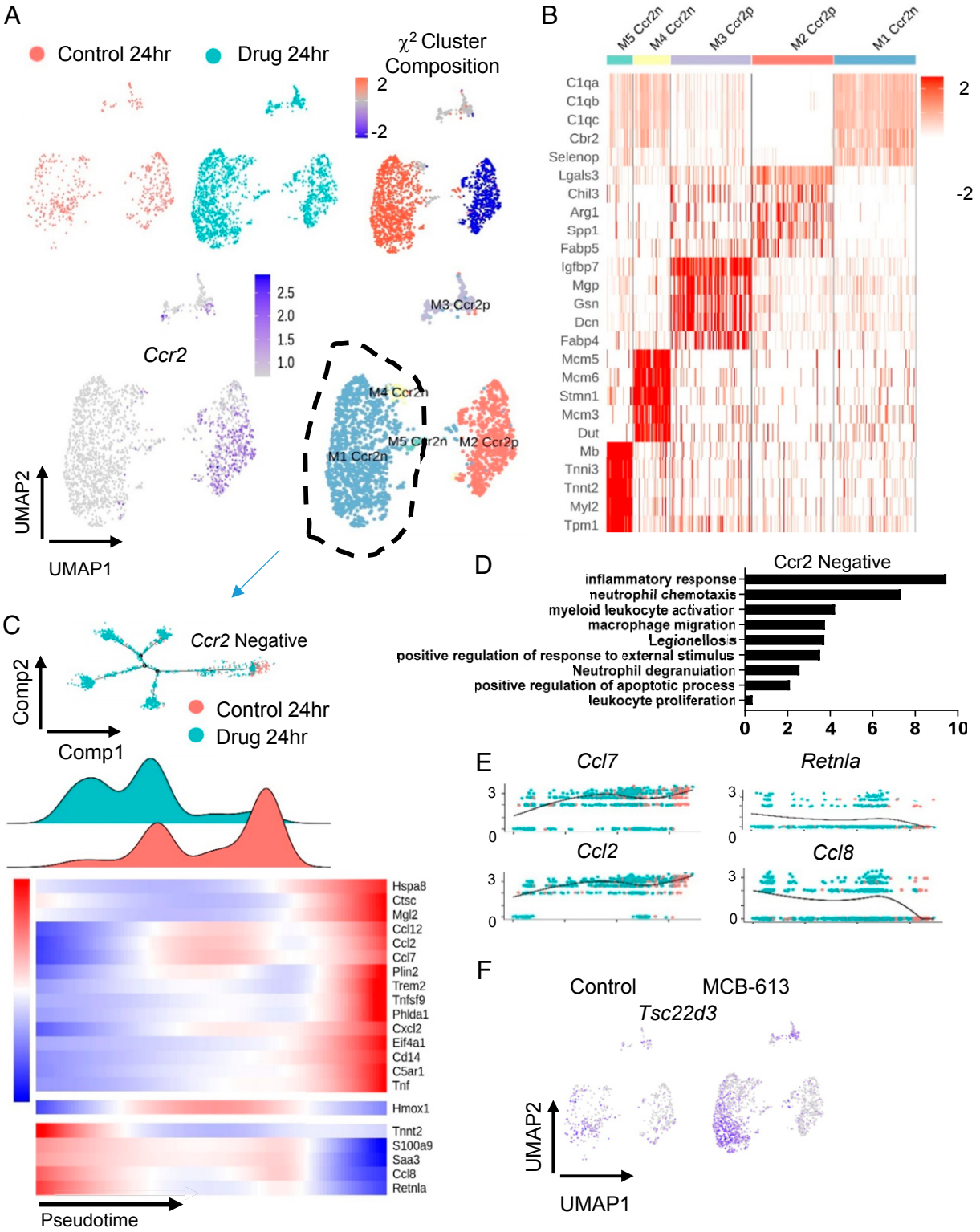

Fig. 4. Single cell analysis of macrophages 24 h post-MI reveals that the MCB-613 protective response is associated with increased anti-inflammatory macrophages and macrophage and granulocyte functions. (*A*) UMAP plot of macrophages from control (salmon) and MCB-613 (aqua) 24 h post-MI. The χ^2 cluster composition analysis of subclustered macrophages from MCB-613 compared to control at 24 h post-MI (*Top Right*). UMAP plot of macrophage subclusters 24 h post-MI (*Bottom Right*). (*B*) Heat map showing top five differentially expressed genes. (*C*) Pseudotime trajectory and density plot of Ccr2n macrophages across the pseudotime trajectory. Heatmap showing dynamics of gene expression for Ccr2n macrophages across the trajectory. (*D*) GO terms analysis of differentially expressed genes from macrophages in control compared to MCB-613. (*E*) Gene expression trends for individual genes across the pseudotime trajectory. (*F*) Feature plot showing *Tsc22d3* expression in macrophages for control and MCB-613.

To determine how the reparative Ccr2 negative macrophages change in response to MCB-613, cell trajectory analysis was performed using differentially expressed genes (Controls vs. MCB-613) as defining factors (Fig. 4*C*). The *Ccr2* negative macrophages from control-treated mice represent a unified group positioned in mid to right sections of the trajectory while macrophages from MCB-613-treated mice branch into four different branches from the left to mid sections. Decreased representation of Ccr2 negative macrophages in right positions indicate MCB-613 suppresses phenotype changes of tissue resident *Ccr2* negative macrophages in response to injury. The trajectory analysis of Ccr2 positive macrophages is in Supporting Information (*SI Appendix*, Fig. S3*B*).

Ccr2 positive macrophages from control MI mice are enriched in the later pseudotime ("differentiated state") 24 h post-MI compared to macrophages in MCB-613-treated mice (*SI Appendix*, Fig. S3). Proinflammatory genes *Spp1* and *Ctsl* are highly expressed in the control Ccr2p macrophages enriched in the late pseudotime population, indicating proinflammatory activation is repressed in injured hearts in response to MCB-613.

We next examined the biological impact of MCB-613 by GO analysis and found inflammatory response as the most represented among the differentially expressed genes (shown in trajectory heatmap) (Fig. 4*D*). Additional biological process impacted include neutrophil chemotaxis and macrophage migration, indicating MCB-613 acts to suppress immune cell recruitment. Gene expression across the trajectory for resident Ccr2 negative macrophages indicates macrophage differentiation 24 h post-MI is associated with expression of *Ccl2* and *Ccl7* inflammatory chemokines (Fig. 4*E*). Genes differentially expressed in the enriched population of Ccr2 negative macrophages include *Ccl8*, a Ccr5 positive helper T cell recruiter (27); *Retnla*, a proreparative alternatively activated macrophage marker (28); and TSC22 domain family member 3 (*Tsc22d3*) (Fig. 4*F*), an anti-inflammatory glucocorticoid (GC)-induced leucine zipper protein previously shown to provide post-MI cardioprotection (29), all potentially contributing to the beneficial response to MCB-613.

Heart tissue sections show a significant increase in TSC22D3 protein expression by IF in the myocardium of MCB-613-treated mice compared to control mice 3 d post-MI (*SI Appendix*, Fig. S4). *Tsc22d3* likely plays an important role in the cardioprotective effects of MCB-613 3 d post-MI. MCB-613 regulation of neutrophil degranulation (Fig. 4*D*) indicates granulocyte and macrophage granules also play a role in MCB-613's post-MI immune regulatory and tissue-remodeling effects. In support of this, LYZ1 granule expression is significantly increased in the myocardium of MCB-613-treated mice compared to control mice 24 h, 3 d, 6 wk, and 12 wk post-MI (*SI Appendix*, Fig. S5). Overall, the data suggest MCB-613 treatment contributes to improved cardiac function 24 h post-MI by establishing a proreparative, anti-inflammatory environment by shifting the macrophage population by enrichment of proreparative Ccr2 negative macrophages and reduction of proinflammatory Ccr2 positive infiltrating macrophages.

MCB-613 Effects on Fibroblasts and Macrophages Are Maintained Long-Term. We explored differences in fibroblast and macrophage clusters 12 wk post-MI. A shift in cell composition indicates MCB-613 maintains a long-lasting change in fibroblast composition 12 wk post-MI (Fig. 5*A* and *SI Appendix*, Fig. S6). Fibroblasts consist of eight major clusters (Fig. 5*B*). Similar to 24 h post-MI, *Lpl*-expressing fibroblasts (CF A) are enriched in hearts from MCB-613-treated mice compared to control, suggesting early effects of MCB-613 on post-MI fibroblasts are maintained in chronic post-MI hearts (Fig. 5 *A* and *B*). The most highly enriched fibroblast population (CF-C) is marked by expression of the matrifibrocyte marker cartilage oligomeric matrix protein (COMP), previously suggested to have an important role in maintaining the structural integrity of post-MI scar tissue (23). Trajectory and density analysis of cardiac fibroblasts 12 wk post-MI predicts smaller clusters CF-B, CF-E, and CF-G are positioned in later pseudotime ("differentiated states"), with major populations CF-A and CF-F in early and middle positions while *Comp* positive fibroblasts (CF-C) are highly enriched only in early pseudotime (Fig. 5 *C* and *D*). Underrepresentation of CF-B fibroblasts characterized by expression of inflammatory cytokines suggests MCB-613 treatment suppresses fibroblast inflammatory signaling 12 wk post-MI (Fig. 5*C*). Enriched COMP-expressing cells have higher levels of *Angptl7*, WNT1-inducible-signaling pathway protein 2 (*Wisp2*), and Wnt pathway inhibitor *Sfrp2* (30), suggesting vascular and Wnt pathway signaling contribute to long-term scar maintenance (Fig. 5 *C* and *D*). In support of this, GO analysis indicates extracellular structure organization, collagen fibril organization and metabolic process, and vasculature late matrix remodeling controls post-MI scar maintenance effects (Fig. 5*E*). Overall, these data indicate MCB-613 actions in the post-MI inflammatory and repair phases promote long-term beneficial scar remodeling.

We next investigated long-term effects of MCB-613 on cardiac macrophages. Macrophages consist of 11 major clusters at 12 wk post-MI, compared to five macrophage clusters 24 h post-MI, indicating increased macrophage cell types are associated with cardiac maintenance 12 wk post-MI, likely a reflection of maturation of the post-MI tissue microenvironment (Fig. 5*F* and *SI Appendix*, Fig. S6). A two-color analysis shows a shift in cell composition indicating MCB-613 affects postinjury macrophage cell types 12 wk post-MI (*SI Appendix*, Fig. S6). Similar to 24 h post-MI, a χ^2 analysis shows *Cbr2* macrophages are enriched 12 wk post-MI, indicating these macrophages also contribute to long-term post-MI effects of MCB-613 (Fig. 5 *G* and *H*).

MCB-613 Promotes Stromal-Immune Cell Paracrine Signaling. To identify potential interstitial cell signaling interactions contributing to improved cardiac function after MCB-613 treatment, we calculated the number of interactions between up and down-regulated ligands and their associated receptors for nonmacrophage-immune, macrophage, endothelial, and fibroblast cells in control hearts compared to hearts from MCB-613-treated mice (31). We first calculated the number of up and down-regulated ligands 24 h post-MI (*SI Appendix*, Fig. S7*A*). We next examined GO terms and found inflammatory response as the most overrepresented in differentially expressed up-regulated ligands and leukocyte migration for down-regulated ligand genes at 24 h post-MI suggesting early inflammatory signaling controls post-MI immune effects (*SI Appendix*, Fig. S7*B*). Of the regulated cytokines, *Ccl8* ligand expressed in Ccr2 negative macrophages had the highest frequency of up-regulated interactions with nonmacrophage immune cells, endothelial cells, and fibroblasts (*SI Appendix*, Fig. S7 *C*, *Left*). Although the exact role for *Ccl8* in cardiac remodeling is unknown, these data suggest *Ccl8* signaling underlies MCB-613's effects on resident *Ccr2* positive macrophage functions. Evaluation of other ligands shows high frequency signaling between *S100a8* and *S100a9* ligands from the underrepresented Ccr2 positive macrophages and fibroblasts signaling to *Tlr4* receptors, indicating MCB-613 suppresses paracrine inflammatory signaling. The highest frequency of down-regulated ligand-receptor interactions occurred between extracellular matrix (ECM) glycoprotein *Spp1* from macrophages and nonmacrophage immune cells signaling to nonmacrophage immune cells, macrophages, fibroblast integrin, and *Cd44* receptors at 24 h post-MI, indicating diverse cell types contribute to early beneficial ECM remodeling and suppression of immune cell migration in post-MI hearts from MCB-613-treated mice (*SI Appendix*, Fig. S7 *C*, *Right*). This strong pattern of down-regulation of fibrotic and immune cell recruitment signaling between fibroblast and total immune cells implicates extensive paracrine regulation of fibrotic ECM remodeling and inflammatory functions in the MCB-613 cardioprotective response 24 h post-MI.

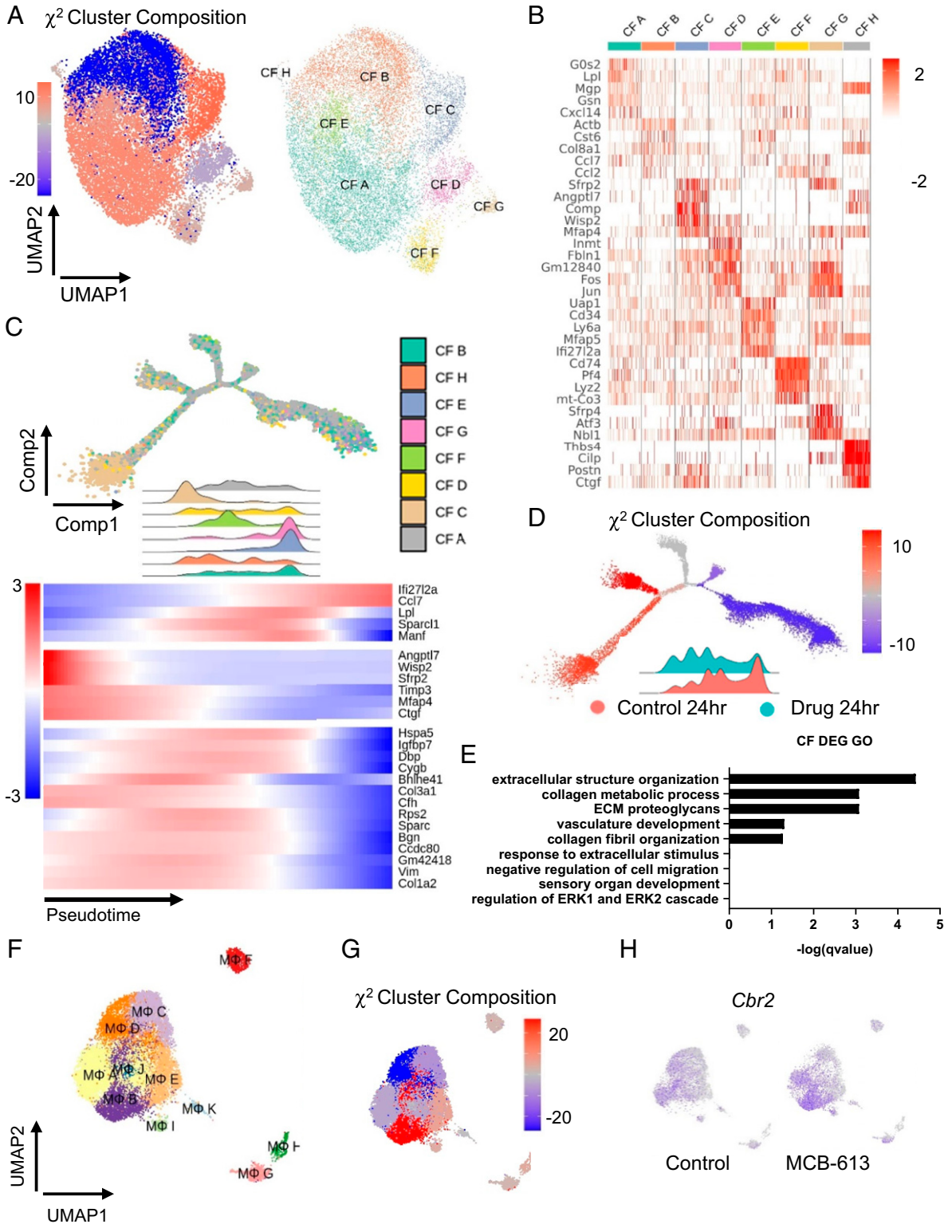

Fig. 5. MCB-613 promotes long-lasting fibroblast differentiation and enrichment of *Cbr2* macrophages. (*A*) χ^2 cluster composition analysis of subclustered fibroblasts 12 wk post-MI (*Left*). UMAP plot of fibroblast subclusters (*Right*). (*B*) Heat map showing top differentially expressed genes. (*C*) Pseudotime trajectory and corresponding density ridge plot across the pseudotime trajectory colored according to cluster identity (*Top*). Heatmap showing dynamics of gene expression for fibroblasts across the trajectory (*Bottom*). (*D*) The χ^2 cluster composition analysis of subclustered fibroblasts across the trajectory. Density ridge plot according to treatment condition. (*E*) GO terms analysis of differentially expressed genes from fibroblasts in control compared to MCB-613. (*F*) UMAP plot of macrophage subclusters 12 wk post-MI. (*G*) The χ^2 cluster composition analysis of subclustered macrophages from MCB-613 compared to control 12 wk post-MI. (*H*) *Cbr2* expression feature plot.

MCB-613 Regulates Inflammatory and Fibrotic Signaling Responses In Vitro. Given the evidence that MCB-613 decreases inflammatory transcriptional responses in immune cells and fibroblasts 24 h post-MI, we measured the effect of MCB-613 on immune cells and fibroblasts. Specifically, we sought to examine the acute granulocyte transcriptional response to MCB-613 due to the overrepresentation of a degranulation response and increased LYZ1 protein in hearts 24 h post-MI. Granulocytes are the first innate immune cells to reach the myocardium after acute ischemic injury and are critical mediators of the inflammatory reaction triggered by an acute MI and of the resulting damage to the heart muscle. Due to the difficulty of isolating sufficient quantities of undamaged granulocytes from mouse hearts, we isolated bone marrow granulocytes from MI mice 24 h post-MI, which reflect the early granulocyte response (32). Elevated messenger RNA (mRNA) expression of the granulocyte marker *S100A9* in granulocytes compared to granulocyte-depleted bone marrow indicated successful isolation of granulocytes (Fig. 6*A*). Increased expression of *Tlr7* and *Lcn2* in granulocytes from mice treated with MCB-613 reveals that modulation of granule functions contributes to the acute myocardial response to MCB-613.

The increase in macrophage cell numbers and their involvement in cell-cell signaling 24 h post-MI indicates that MCB-613 may also play a transcriptional role in macrophage cell responses. To test the ability of MCB-613 to regulate macrophages, murine-derived RAW 264.7 macrophage cells were treated with MCB-613 and/or proinflammatory M1 factors to investigate the effect of MCB-613 on gene expression in resting macrophages or macrophages undergoing reprogramming. MCB-613 had no effect on inflammatory gene expression in resting macrophages (*SI Appendix*, Fig. S8). However, MCB-613 significantly repressed *Il-1b*, *Tnf-α*, *Ccl4*, *Spp1, Cxcl19*, and *IL-6* mRNA expression in the presence of M1 factors, indicating that MCB-613 reduces proinflammatory macrophage functions (Fig. 6*B*). Modulation of macrophage inflammatory cytokine genes in vitro suggests MCB-613 controls both direct and paracrine post-MI inflammatory processes.

We sought to investigate the effects of MCB-613 on stromal responses specifically in adult cardiac fibroblasts. SRC-1, 2, and 3 proteins are expressed in adult cardiac fibroblasts isolated from 10 wk old mice (Fig. 6*C*). Cardiac fibroblasts were transfected with expression vectors for GAL4 DNA binding domain-SRC-1, 2, and 3 fusion proteins and a GA4-responsive luciferase reporter to measure SRC activation following MCB-613 treatment (Fig. 6*C*). SRC-3 activity is induced in response to MCB-613 to a greater extent than for SRC-1 and SRC-2, indicating that MCB-613 preferentially stimulates SRC-3 activity in cardiac fibroblasts. To investigate MCB-613's stimulation of fibroblast gene expression, RT-qPCR was performed in cardiac fibroblasts treated with MCB-613 or vehicle control. Twenty-four hours following administration of MCB-613, expression of the matricellular protein *Ctgf* along with IL-1 response genes *Saa3*, *Serpine1*, and *Ccl2* are decreased (Fig. 6*D*). These findings support the decreased representation of the injury-reactive fibroblast response by single cell analysis and further indicate that MCB-613 stimulation of cardiac fibroblasts functions to suppress fibrotic and IL-1 inflammatory responses. Modulation of fibrotic and IL-1 response genes in vitro suggests MCB-613 controls both direct and paracrine fibroblast functions. Together, these data indicate MCB-613 functions on immune signaling together with fibroblast IL-1 and matricellular responses play critical roles in the early post-MI ischemic response.

Discussion

The adult human heart has limited regenerative capacity following MI due to its homeostatic response to maintain cardiovascular integrity by replacing lost cardiomyocytes with a collagenous scar (33). Although immediately advantageous in maintaining cardiac structural integrity, continued expansion of scar deposition and remodeling over time leads to loss of cardiac compliance and contractility. Congestive heart failure ensues when this expanding scar limits the heart's pumping volume/capacity to the point that it cannot meet the body's circulatory demands. Current therapeutic approaches to prevent or reverse scar formation often can result in increased risk of cardiac rupture (24, 34). Because of the balance between the need to protect cardiac tissue structural integrity and contractility post-MI, effective therapeutic interventions must act quickly to sustain cardiomyocyte viability while limiting the spread of nonfunctioning scar tissue. This study demonstrates that administration of a single therapeutic chemical immediately following acute ischemic cardiac injury acts to preserve functional myocardium and attenuate detrimental, fibrotic and inflammatory remodeling of the heart.

Pleiotropic Effects of MCB-613 in Cardiac Repair. Single cell analysis reveals MCB-613 cardioprotection following MI involves dynamic remodeling of the ischemic injury cellular response. Early events include suppression of fibroblast differentiation along with suppression of inflammatory macrophages and enrichment of *Ccr2* negative tissue resident macrophages. These findings suggest that in addition to suppression of fibroblasts that cause fibrosis and diastolic dysfunction in heart failure, MCB-613-stimulated anti-inflammatory macrophages contribute to regulation of post-MI injury responses. While cardiomyocytes were not included in the single cell analysis, it is possible MCB-613 actions on cardiomyocyte survival could also limit adverse remodeling post-MI.

Early MCB-613-mediated signaling response pathways regulated in the mouse MI model suggest, at least in part, that IL-1 signaling, immune cell degranulation, and anti-inflammatory immune cells control the ischemic injury response in MCB-613's presence. Early immune regulation by SRCs likely contributes to salvage of vulnerable myocardium and subsequent repair. In mouse cardiac fibroblasts, although all SRCs are expressed, MCB-613 preferentially stimulated SRC-3 activity. Fibroblasts not only function as support cells, they also actively control immune responses. Our data indicate that early suppression of IL-1 signaling is part of the mechanism by which MCB-613 attenuates post-MI fibroblast transdifferentiation and improves heart function post-MI. SRC-3 is known to act as a translational repressor of IL-1beta in lipopolysaccharide (LPS)-stimulated macrophages (14). In vitro studies indicate that IL-1 treatment leads to a proinflammatory, proangiogenic, ECM-degrading phenotype in fibroblasts (35). The control of paracrine IL-1/fibroblast signaling post-MI has been previously shown to regulate post-MI remodeling and improve cardiac function in animal models (36, 37). Results from the CANTOS cardiovascular clinical trial indicates therapeutic blockade of IL-1 reduces cardiovascular events in patients with atherosclerotic vascular disease (reviewed in (38, 39)). Additional paracrine pathways identified indicate *Spp1* and *Serpine1* signaling pathways may be involved in the primary beneficial effect underlying the MCB-613 response in post-MI injured hearts. In support of this, we show MCB-613 decreases fibroblast expression of *Serpine1* and macrophage expression of *Spp1*. These results are consistent with recent reports demonstrating critical roles for *Spp1* and *Serpine1* in cardiac fibrosis and remodeling (40, 41). Our results reveal an essential function of SRC activation in suppressing the early IL-1beta inflammatory response leading to protection against progressive damage post-MI.

Suppression of inflammatory macrophage infiltration and the early increase in anti-inflammatory macrophages indicate that immunomodulation of proinflammatory cytokines and granule functions in the inflammatory phase may limit inflammatory damage while promoting subsequent healing. The significant increase in macrophage numbers along with robust increases in granule gene and protein expression in response to our tool drug MCB-613 (and our patentable derivatives), warrant further future investigations of macrophage and granulocyte biology in the

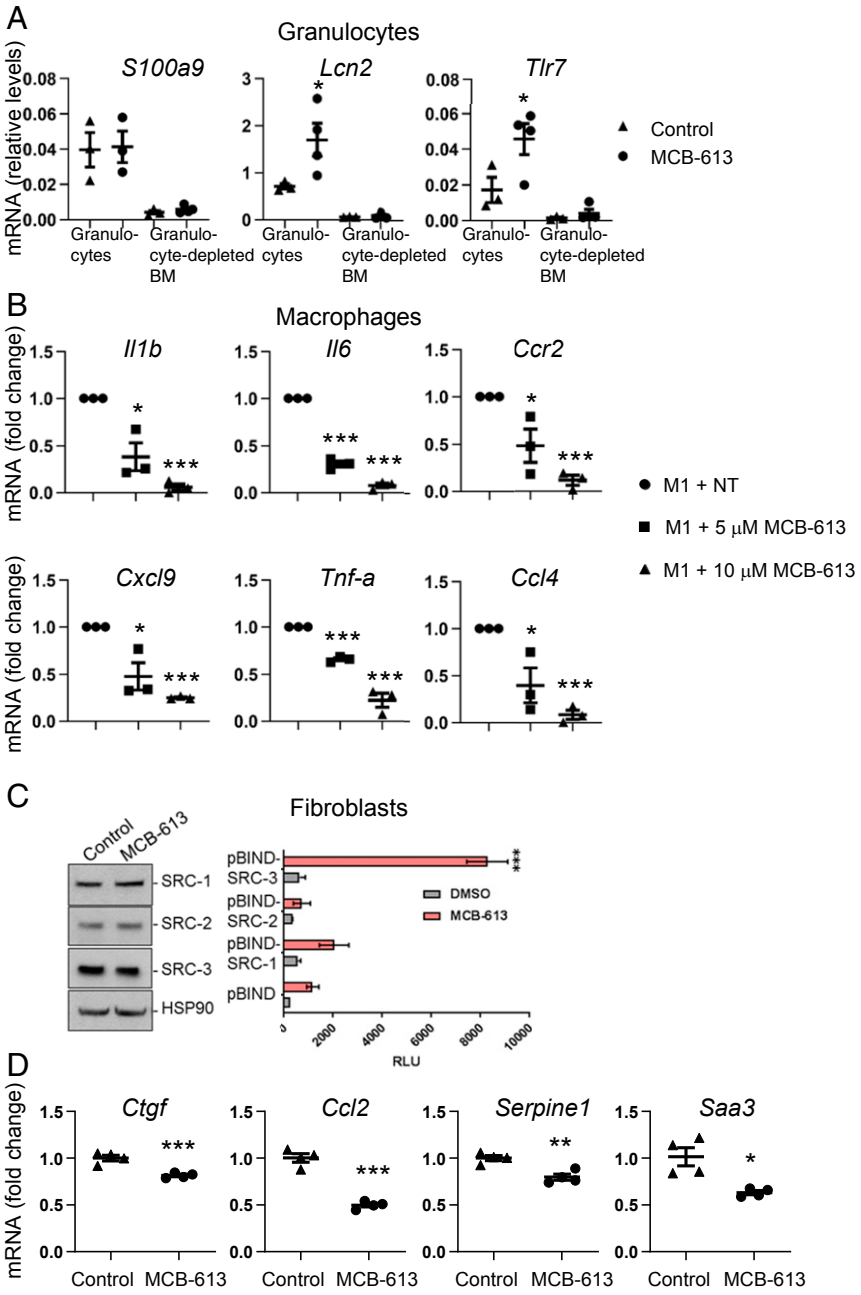

Fig. 6. MCB-613 promotes granulocyte functions and reduces proinflammatory signaling in macrophages and fibroblasts. (*A*) mRNA expression in granulocytes isolated from bone marrow 24 h post-MI and MCB-613 treatment. Gene expression changes in *S100a9*, *Tlr7*, and *Lcn2* were measured by qPCR and 18s RNA expression was used as a control. Values shown are mean ± SEM ($n = 10$ control group, $n = 12$ MCB-613 group); Student's *t* test (*Tlr7* $^*P = 0.01$, *Lcn2* $^*P = 0.04$). (*B*) mRNA expression in RAW 264.7 macrophages stimulated with M1 reprogramming factors for 8 h followed by vehicle control or MCB-613 for an additional 24 h. Values shown are mean ± SEM ($n = 3$ control group, $n = 3$, 5 μM MCB-613 group, $n = 3$, 10 μM MCB-613 group); Student's *t* test (Il1B $^*P = 0.01$, $^{***}P\ 1.3 \times 10^{-5}$; Il6 $^{***}P = 2.9 \times 10^{-5}$, $^{***}P = 3.1 \times 10^{-6}$; Spp1 $^*P = 3.0 \times 10^{-3}$, $^{***}P = 2.4 \times 10^{-4}$, Tnf-α $^{***}P = 3.3 \times 10^{-5}$, $^{***}P = 5.0 \times 10^{-4}$; Ccl4 $^*P = 0.03$, $^{***}P = 4.8 \times 10^{-5}$; Cxcl9 $^*P = 0.02$, $^{***}P = 6.9 \times 10^{-8}$. (*C*) Cardiac fibroblasts were treated with dimethylsulfoxide (DMSO) or MCB-613 for 24 h and protein was immunoblotted for SRC-1, -2, and -3. Cardiac fibroblasts were transfected with a GAL4 DNA binding site-luciferase reporter (pG5-luc) and GAL4-DNA binding domain-full-length SRC-1, -2, or -3 fusion (pBIND-SRC) or control pBIND expression vectors. Posttransfection, the cells were treated with DMSO or MCB-613 for 24 h. Values shown are mean ± SEM of a representative experiment repeated three times; Student's *t* test ($^{***}P < 0.00001$). (*D*) RT-PCR of mRNA isolated from cardiac fibroblasts 24 h after treatment with control or MCB-613. mRNA fold change for representative of three experiments, values shown are mean ± SEM $n = 4$ control group, $n = 4$, 5 μM MCB-613. *Serpine1* $P = 0.003$, *Ctgf* $P = 0.001$, *Ccl2* $P = 0.0001$, *Saa3* $P = 0.009$.

cardiac injury response. For example, maintenance of increased *Cbr2* positive macrophages 12 wk post-MI indicates *Cbr2* macrophage functions may play a role in long-term maintenance of post-MI fibrosis and scar remodeling.

The mechanisms of SRC regulation of targets involved in stromal and immune responses expressed in the post-MI myocardium, including NF-κB (42), Mef2c (43), and Vegfr2 (18, 44), have been well defined. In the cardiovascular system of adult mice, expression of either SRC-1 or SRC-3 in vascular smooth muscle cells and endothelial cells is required for protective effects of estrogen on the vascular injury response (45, 46). In mouse embryonic development, knock-out of both SRC-1 and SRC-3 resulted in reduced

fetal vascular development followed by embryonic lethality at E13.5, likely through modulation of FGF expression (17). In support of this, the FGF chaperone and angiogenic factor, fibroblast growth factor binding protein (FGFBP1) is regulated by SRC-3 (47, 48). In vitro, SRC-3 has been shown to integrate ERK3 signaling to promote endothelial cell migration, proliferation, and tube formation by up-regulating SRC-3/CREB-binding protein (CBP)/SP1 transcription factor (SP-1)-mediated VEGF2 expression (44).

Accumulating evidence suggests SRC expression and activation exhibit control over inflammatory networks and physiologic outcomes in a cell and context-specific manner. SRC-3 can control immune functions by working with a number of immune target transcription factors such as interferon (IFN) regulatory factors (IRFs) and NF-κB (10, 49). In mouse models of inflammation and wound healing, SRC-3 acts to suppress NF-κB activation (31), IL1b expression (14), and is required for immune cell recruitment in healing wounds (50). A unique mechanism was identified whereby, in our heart model, we show MCB-613 promotes early enrichment of the glucocorticoid-induced *Tsc22d3* mRNA 24 h post-MI and TSC22D3 protein in the myocardium in the reparative phase 3 d post-MI. Glucocorticoids are essential for cellular stress responses and for treatment of autoimmune and inflammatory conditions. Recent studies suggest glucocorticoid agonists may provide an approach for treating heart disease (51). *Tsc22d3* is a direct target of glucocorticoid receptor and recent evidence indicates *Tsc22d3* attenuates inflammation by inhibition of NF-κB (52); this suggests that MCB-613 may attenuate inflammation without the severe negative side effects of glucocorticoid treatment. Our data indicate therapeutic stimulation of SRCs may provide an approach in constraining the inflammatory signaling in response to ischemic injury.

Recent single cell and genetic lineage-tracing studies have characterized the dynamic expansion and differentiation of resident cardiac fibroblasts in response to myocardial injury. Our study showed that cardiac resident *Lpl*-expressing fibroblasts are enhanced 24 h post-MI in response to MCB-613. Demonstration that *Lpl* positive fibroblasts are similarly enhanced 12 wk post-MI suggests MCB-613 promotes expansion or survival of resident fibroblasts. Enrichment of COMP positive fibroblasts 12 wk post-MI indicates MCB-613 actions simply do not mitigate damage but also contribute to scar remodeling and maintenance. A recent study demonstrated the differentiation of resident fibroblasts into long-lasting matrifibrocytes occurs by day 10 within the post-MI scar region (23). MCB-613 promotion of matrifibrocyte-like fibroblasts indicates lasting protection is associated with improved structural integrity that likely occurred by day 7 post-MI. Although genetic lineage tracing is required to confirm, our data suggest early MCB-613 promotion of matrifibrocyte-like fibroblast differentiation protects hearts from progressive damage post-MI, leading to long-term maintenance of cardiac function.

In summary, treatment with MCB-613 (and its unique derivatives) immediately after ischemic injury can attenuate both early and chronic loss of cardiac function after an MI. Our results indicate MCB-613 controls the cellular interstitial cardiac repair response to ischemia by coordinately regulating multiple key factors involved in the cardiac ischemic injury response; it occurs in part by its intrinsic and powerful transcriptional growth and repair effects on numerous nuclear genes in multiple cell types. Furthermore, distinct molecular and cellular mechanisms related to stimulation of SRC-3 have been identified that pave the way for the further exploration of SRCs as drug targets that can be engaged to improve the management of myocardial injury response outcomes.

Materials and Methods

Detailed material and methods for the reporter assay, model of heart failure in adult mice, echocardiography, histological analysis, electron microscopy, isolation of cardiac cells, single cell RNA-seq analysis, granulocyte isolation, Western blots, immunostaining, RAW264.7 treatment with MCB-613, qPCR, VO_2 and VCO_2 measurements, statistics, and study approval are described in the *SI Appendix*.

Data Availability. Single cell RNA sequencing data have been deposited in Gene Expression Omnibus database (accession no. GSE157542). All study data are included in the article and *SI Appendix*.

ACKNOWLEDGMENTS. Acknowledgments are provided in the *SI Appendix*.

1. X. Chen *et al.*, Knockout of SRC-1 and SRC-3 in mice decreases cardiomyocyte proliferation and causes a noncompaction cardiomyopathy phenotype. *Int. J. Biol. Sci.* **11**, 1056–1072 (2015).
2. J. H. Suh *et al.*, Steroid receptor coactivator-2 (SRC-2) coordinates cardiomyocyte paracrine signaling to promote pressure overload-induced angiogenesis. *J. Biol. Chem.* **292**, 21643–21652 (2017).
3. L. Wang *et al.*, Characterization of a steroid receptor coactivator small molecule stimulator that overstimulates cancer cells and leads to cell stress and death. *Cancer Cell* **28**, 240–252 (2015).
4. D. M. Lonard, B. W. O'malley, Nuclear receptor coregulators: Judges, juries, and executioners of cellular regulation. *Mol. Cell* **27**, 691–700 (2007).
5. R. B. Lanz *et al.*, Global characterization of transcriptional impact of the SRC-3 coregulator. *Mol. Endocrinol.* **24**, 859–872 (2010).
6. M. Percharde *et al.*, Ncoa3 functions as an essential Esrrb coactivator to sustain embryonic stem cell self-renewal and reprogramming. *Genes Dev.* **26**, 2286–2298 (2012).
7. A. D. Rohira *et al.*, Targeting SRC coactivators blocks the tumor-initiating capacity of cancer stem-like cells. *Cancer Res.* **77**, 4293–4304 (2017).
8. J. Xu *et al.*, The steroid receptor coactivator SRC-3 (p/CIP/RAC3/AIB1/ACTR/TRAM-1) is required for normal growth, puberty, female reproductive function, and mammary gland development. *Proc. Natl. Acad. Sci. U.S.A.* **97**, 6379–6384 (2000).
9. B. York, B. W. O'Malley, Steroid receptor coactivator (SRC) family: Masters of systems biology. *J. Biol. Chem.* **285**, 38743–38750 (2010).
10. R. C. Wu *et al.*, Regulation of SRC-3 (pCIP/ACTR/AIB-1/RAC-3/TRAM-1) Coactivator activity by I kappa B kinase. *Mol. Cell. Biol.* **22**, 3549–3561 (2002).
11. S. Dasgupta *et al.*, Coactivator SRC-2-dependent metabolic reprogramming mediates prostate cancer survival and metastasis. *J. Clin. Invest.* **125**, 1174–1188 (2015).
12. Q. Su *et al.*, Role of AIB1 for tamoxifen resistance in estrogen receptor-positive breast cancer cells. *Oncology* **75**, 159–168 (2008).
13. J. Yan *et al.*, Steroid receptor coactivator-3/AIB1 promotes cell migration and invasiveness through focal adhesion turnover and matrix metalloproteinase expression. *Cancer Res.* **68**, 5460–5468 (2008).
14. C. Yu *et al.*, An essential function of the SRC-3 coactivator in suppression of cytokine mRNA translation and inflammatory response. *Mol. Cell* **25**, 765–778 (2007).
15. L. Qin *et al.*, NCOA1 promotes angiogenesis in breast tumors by simultaneously enhancing both HIF1α- and AP-1-mediated VEGFa transcription. *Oncotarget* **6**, 23890–23904 (2015).
16. B. York *et al.*, Research resource: Tissue- and pathway-specific metabolomic profiles of the steroid receptor coactivator (SRC) family. *Mol. Endocrinol.* **27**, 366–380 (2013).
17. X. Chen, Z. Liu, J. Xu, The cooperative function of nuclear receptor coactivator 1 (NCOA1) and NCOA3 in placental development and embryo survival. *Mol. Endocrinol.* **24**, 1917–1934 (2010).
18. E. L. Reineke *et al.*, Steroid receptor coactivator-2 is a dual regulator of cardiac transcription factor function. *J. Biol. Chem.* **289**, 17721–17731 (2014).
19. E. Ubil *et al.*, Mesenchymal-endothelial transition contributes to cardiac neovascularization. *Nature* **514**, 585–590 (2014).
20. M. D. Tallquist, J. D. Molkentin, Redefining the identity of cardiac fibroblasts. *Nat. Rev. Cardiol.* **14**, 484–491 (2017).
21. T. Heallen *et al.*, Hippo signaling impedes adult heart regeneration. *Development* **140**, 4683–4690 (2013).
22. E. Becht *et al.*, Dimensionality reduction for visualizing single-cell data using UMAP. *Nat. Biotechnol.*, 10.1038/nbt.4314 (2018).
23. X. Fu *et al.*, Specialized fibroblast differentiated states underlie scar formation in the infarcted mouse heart. *J. Clin. Invest.* **128**, 2127–2143 (2018).
24. A. V. Shinde, N. G. Frangogiannis, Fibroblasts in myocardial infarction: A role in inflammation and repair. *J. Mol. Cell. Cardiol.* **70**, 74–82 (2014).
25. N. Farbehi *et al.*, Single-cell expression profiling reveals dynamic flux of cardiac stromal, vascular and immune cells in health and injury. *eLife* **8**, e43882 (2019).
26. G. Bajpai *et al.*, Tissue resident CCR2- and CCR2+ cardiac macrophages differentially orchestrate monocyte recruitment and fate specification following myocardial injury. *Circ. Res.* **124**, 263–278 (2019).
27. G. F. Debes, M. C. Diehl, CCL8 and skin T cells–An allergic attraction. *Nat. Immunol.* **12**, 111–112 (2011).
28. M. Shiraishi *et al.*, Alternatively activated macrophages determine repair of the infarcted adult murine heart. *J. Clin. Invest.* **126**, 2151–2166 (2016).
29. B. Baban *et al.*, The role of GILZ in modulation of adaptive immunity in a murine model of myocardial infarction. *Exp. Mol. Pathol.* **102**, 408–414 (2017).

30. C. M. Cruciat, C. Niehrs, Secreted and transmembrane wnt inhibitors and activators. *Cold Spring Harb. Perspect. Biol.* **5**, a015081 (2013).
31. J. A. Ramilowski *et al*., A draft network of ligand-receptor-mediated multicellular signalling in human. *Nat. Commun.* **6**, 7866 (2015).
32. X. Wang *et al*., Donor myocardial infarction impairs the therapeutic potential of bone marrow cells by an interleukin-1-mediated inflammatory response. *Sci. Transl. Med.* **3**, 100ra90 (2011).
33. M. G. Sutton, N. Sharpe, Left ventricular remodeling after myocardial infarction: Pathophysiology and therapy. *Circulation* **101**, 2981–2988 (2000).
34. S. W. van den Borne *et al*., Myocardial remodeling after infarction: The role of myofibroblasts. *Nat. Rev. Cardiol.* **7**, 30–37 (2010).
35. N. A. Turner, Effects of interleukin-1 on cardiac fibroblast function: Relevance to post-myocardial infarction remodelling. *Vascul. Pharmacol.* **60**, 1–7 (2014).
36. S. A. Bageghni *et al*., Fibroblast-specific deletion of interleukin-1 receptor-1 reduces adverse cardiac remodeling following myocardial infarction. *JCI Insight* **5**, e125074 (2019).
37. M. Bujak *et al*., Interleukin-1 receptor type I signaling critically regulates infarct healing and cardiac remodeling. *Am. J. Pathol.* **173**, 57–67 (2008).
38. L. F. Buckley *et al*., Effect of interleukin-1 blockade on left ventricular systolic performance and work: A post hoc pooled analysis of 2 clinical trials. *J. Cardiovasc. Pharmacol.* **72**, 68–70 (2018).
39. P. Libby, Interleukin-1 beta as a target for Atherosclerosis Therapy: Biological basis of CANTOS and Beyond. *J. Am. Coll. Cardiol.* **70**, 2278–2289 (2017).
40. I. Abdelaziz Mohamed, A. P. Gadeau, A. Hasan, N. Abdulrahman, F. Mraiche, Osteopontin: A promising therapeutic target in cardiac fibrosis. *Cells* **8**, 1558 (2019).
41. P. E. Morange *et al*., Association of plasminogen activator inhibitor (PAI)-1 (SERPINE1) SNPs with myocardial infarction, plasma PAI-1, and metabolic parameters: The HIFMECH study. *Arterioscler. Thromb. Vasc. Biol.* **27**, 2250–2257 (2007).
42. A. Coste *et al*., Absence of the steroid receptor coactivator-3 induces B-cell lymphoma. *EMBO J.* **25**, 2453–2464 (2006).
43. S. L. Chen, D. H. Dowhan, B. M. Hosking, G. E. Muscat, The steroid receptor coactivator, GRIP-1, is necessary for MEF-2C-dependent gene expression and skeletal muscle differentiation. *Genes Dev.* **14**, 1209–1228 (2000).
44. W. Wang *et al*., ERK3 promotes endothelial cell functions by upregulating SRC-3/SP1-mediated VEGFR2 expression. *J. Cell. Physiol.* **229**, 1529–1537 (2014).
45. Y. Yuan, L. Liao, D. A. Tulis, J. Xu, Steroid receptor coactivator-3 is required for inhibition of neointima formation by estrogen. *Circulation* **105**, 2653–2659 (2002).
46. Y. Yuan, J. Xu, Loss-of-function deletion of the steroid receptor coactivator-1 gene in mice reduces estrogen effect on the vascular injury response. *Arterioscler. Thromb. Vasc. Biol.* **27**, 1521–1527 (2007).
47. V. K. Harris *et al*., Induction of the angiogenic modulator fibroblast growth factor-binding protein by epidermal growth factor is mediated through both MEK/ERK and p38 signal transduction pathways. *J. Biol. Chem.* **275**, 10802–10811 (2000).
48. T. Lahusen, M. Fereshteh, A. Oh, A. Wellstein, A. T. Riegel, Epidermal growth factor receptor tyrosine phosphorylation and signaling controlled by a nuclear receptor coactivator, amplified in breast cancer 1. *Cancer Res.* **67**, 7256–7265 (2007).
49. D. A. Rollins, M. Coppo, I. Rogatsky, Minireview: Nuclear receptor coregulators of the p160 family: Insights into inflammation and metabolism. *Mol. Endocrinol.* **29**, 502–517 (2015).
50. M. Al-Otaiby *et al*., Role of the nuclear receptor coactivator AIB1/SRC-3 in angiogenesis and wound healing. *Am. J. Pathol.* **180**, 1474–1484 (2012).
51. R. H. Oakley *et al*., Cardiomyocyte glucocorticoid and mineralocorticoid receptors directly and antagonistically regulate heart disease in mice. *Sci. Signal.* **12**, eaau9685 (2019).
52. J. Hoppstädter *et al*., Induction of glucocorticoid-induced leucine zipper (GILZ) contributes to anti-inflammatory effects of the natural product curcumin in macrophages. *J. Biol. Chem.* **291**, 22949–22960 (2016).